Interface and confined optic phonon modes for superlattices in the long-wavelength limit

1993 J. Phys.: Condens. Matter 5 2919

(http://iopscience.iop.org/0953-8984/5/18/014)

J. Phys.: Condens. Matter 5 (1993) 2919–2926. Printed in the UK

Interface and confined optic phonon modes for superlattices in the long-wavelength limit

T Dumelow and S R P Smith

Department of Physics, University of Essex, Wivenhoe Park, Colchester, Essex CO4 3SQ, UK

Received 26 October 1992

Abstract. The macroscopic dielectric function of a superlattice is used to describe the angular dependence of the superlattice's confined phonons and their associated polaritons at long wavelengths. Results are shown for short-period GaAs/AlAs superlattices making use of a dielectric tensor derived from a linear chain model that can take account of the effects of interface roughness. The method gives a unified description of interface and confined optic phonon modes in the long-wavelength limit, and provides precise information about the angular dependence of mode frequencies that are accessible to micro-Raman and far infrared measurements.

1. Introduction

Interface (IF) polaritons in superlattices have been well known for a long time, and calculation of their dispersion properties has been a straightforward matter when considering alternative layers of thick bulk materials. In the case of a superlattice of alternating layers of thicknesses d_1 and d_2 and dielectric functions $\epsilon_1(\omega)$ and $\epsilon_2(\omega)$, grown along the z axis, the dispersion relation for unretarded modes takes the form [1,2]

$$\cos\left[q_z(d_1+d_2)\right] = \cosh(q_x d_1)\cosh(q_x d_2) + \tfrac{1}{2}(\epsilon_1/\epsilon_2 + \epsilon_2/\epsilon_1)\sinh(q_x d_1)\sinh(q_x d_2). \tag{1}$$

Electromagnetic IF modes of this type have an overall wavevector of the form $(q_x, 0, q_z)$ and the local amplitudes of the fields have maxima at the interfaces and fall off exponentially from the interfaces with a decay constant q_x. Thus q_x serves both as a macroscopic parameter for the whole superlattice and as a local wavevector within each layer, whilst q_z is a Bloch wavevector which is only applicable to the macroscopic propagation.

Recent micro-Raman experiments [3–5] have permitted a study of modes of this type in semiconductor superlattices. However, the IF polaritons encountered in short-period superlattices are somewhat more complex than the situation represented by (1), most notably due to the presence of phonon confinement [5] and interface roughness. Lattice dynamical calculations [6–8] for such modes are complicated due to the three-dimensional nature of the problem, and this has prompted a number of investigations in a continuum approximation [9, 10]. Use of such approximations in a manner which accurately mirrors the behaviour expected from microscopic models has not proved trivial, however, although simple models which show the basic features are now being reported [11, 12].

However, at long wavelengths an alternative and very simple approach to this problem can be applied through the use of the macroscopic dielectric functions, as described by Chu and co-workers [13, 14]. In this paper we illustrate the use of this approach with particular

0953-8984/93/182919+08$07.50

reference to short-period GaAs/AlAs superlattice dielectric functions calculated using the linear chain model of Samson *et al* [15, 16]. This model also permits the inclusion of the effects of interface roughness.

2. Macroscopic phonon and unretarded interface modes

In the long wavelength limit, the dielectric properties of a superlattice may be represented by considering the structure as a single uniaxial medium. The simplest treatment, the bulk slab model, is applicable to long-period superlattices in which confinement effects may be ignored, and gives the principal components of the resulting dielectric tensor in the form [17, 18]

$$\epsilon_{xx} = \epsilon_{yy} = (\epsilon_1 d_1 + \epsilon_2 d_2)/(d_1 + d_2) \tag{2}$$

$$\epsilon_{zz}^{-1} = (\epsilon_1^{-1} d_1 + \epsilon_2^{-1} d_2)/(d_1 + d_2) \tag{3}$$

In a short-period superlattice, the effects of confinement cannot be ignored. Each principal component of the dielectric tensor then contains a series of resonances at the appropriate confined mode frequencies. If damping terms are ignored, they take the form [14]

$$\epsilon_{xx} = \epsilon_{yy} = \epsilon_{\infty xx}\left(1 - \sum_{\mu} \frac{R_{T\mu}}{\omega^2 - \omega_{T\mu}^2}\right) \tag{4}$$

$$\frac{1}{\epsilon_{zz}} = \frac{1}{\epsilon_{\infty zz}}\left(1 + \sum_{\mu} \frac{R_{L\mu}}{\omega^2 - \omega_{L\mu}^2}\right) \tag{5}$$

where $\omega_{T\mu}$ and $\omega_{L\mu}$ are the frequencies of the confined TO and LO phonons and $R_{T\mu}$ and $R_{L\mu}$ are their oscillator strengths. $\epsilon_{\infty xx}$ and $\epsilon_{\infty zz}$ are the principal components of the high-frequency dielectric function. The summation over μ covers all phonon modes in the phonon bands of both constituents. The values of the various parameters depend on the confinement model employed. For a superlattice containing interface roughness the dielectric tensor may still be represented by (4) and (5), but the roughness affects the mode parameters [16].

With a superlattice described as a uniaxial medium of the form represented by (2) and (3) or by (4) and (5), it is a simple matter to apply standard propagation expressions. Thus p-polarization propagation in the x–z plane is represented by

$$q_x^2/\epsilon_{zz} + q_z^2/\epsilon_{xx} = \omega^2/c^2. \tag{6}$$

We now seek phonon-like solutions to (6) by taking the unretarded limit $c \to \infty$, so that the right hand side of (6) vanishes. We consider propagation in which the overall wavevector makes an angle θ with the z axis, i.e. $\tan\theta = q_x/q_z$. Then (6) becomes

$$\tan^2\theta = -\epsilon_{zz}/\epsilon_{xx}. \tag{7}$$

Chu, Ren and Chang [13] describe modes satisfying (7) as anisotropic phonons, and this is indeed a good description in the macroscopic description represented by a dielectric tensor. However, as we shall show, they can also be thought of as long-wavelength IF polaritons, modified by, for instance, phonon confinement or interface roughness.

In order to demonstrate that (7) can represent IF polaritons we consider first the example of a long-period superlattice in which the modes are not perturbed by confinement. In this case we can start by using (1) to represent the IF modes in their unretarded limit. The cos, sinh and cosh terms in this expression may then be expanded as power series. In the long-wavelength limit ($q_z(d_1 + d_2) \ll 1$, $q_x d_1 \ll 1$, $q_x d_2 \ll 1$) the higher-order terms may be ignored. The overall result of this procedure is to produce (7) with ϵ_{xx} and ϵ_{zz} represented by (2) and (3). In the long-wavelength limit, therefore, (1) and (7) are equivalent representations of unretarded IF modes, and either expression could be used to obtain the same result. This is hardly surprising when one considers that the propagation expression used by Raj and Tilley [18] in their derivation of (2) and (3) amounts to (1) in its fully retarded form; they showed that the long-wavelength limit of such an expression is (6) with ϵ_{xx} and ϵ_{zz} defined by (2) and (3) respectively. The two approaches therefore amount to ignoring retardation at different points in the calculation. It is worth mentioning, however, that the method of Raj and Tilley is not the only one that produces equations (2) and (3); Agranovich and Kravtsov [17] arrive at the same result simply by considering average fields over the two layer types and using the appropriate boundary conditions at the interfaces.

The above demonstrates that the same modes can either be described as phonons or unretarded IF polaritons in the bulk slab case. When extra effects such as confinement occur, (7) is still a rigorous description of p-polarized phonons within the long-wavelength limit. Provided the dielectric function is fully modelled, all contributions are automatically included in (7), so that interface contributions need not be separated from those due to confinement.

We can use a similar analysis to that used for deriving (7) to represent s-polarization modes. The s-polarization analogue to (6) is

$$\left(q_x^2 + q_z^2\right)/\epsilon_{xx} = \omega^2/c^2. \tag{8}$$

In a similar manner to the p-polarizations case, in the non-retarded limit the right hand side of (8) disappears. The only solution corresponding to both q_x and q_z real is therefore

$$\epsilon_{xx} \to \infty \tag{9}$$

which occurs at TO modes. Thus phonon modes in s polarization are not anisotropic.

3. Application to linear chain model

The strength of using (7) and (9) to represent the anisotropy of the modes is that the equations can be used with any superlattice model that yields a dielectric function. Such a model may be either continuum or microscopic in nature, and in principle may include extra effects such as plasmons. Derivation of dielectric functions from a linear chain microscopic model is problematic because the long-range forces cannot be explicitly incorporated in a straightforward way, however. Samson *et al* [15, 16] evade this problem by using only effective short-range (nearest and next-nearest neighbour) force constants applicable either to longitudinal or to transverse vibrations, but not to both simultaneously. Overall superlattice dielectric functions which take the same form as (4) and (5) can be obtained from such a model by making use of effective ionic charges obtained from bulk LO–TO splittings. These dielectric functions, although derived from a linear chain model, fully describe electromagnetic propagation, in the long-wavelength limit, in any direction. A further

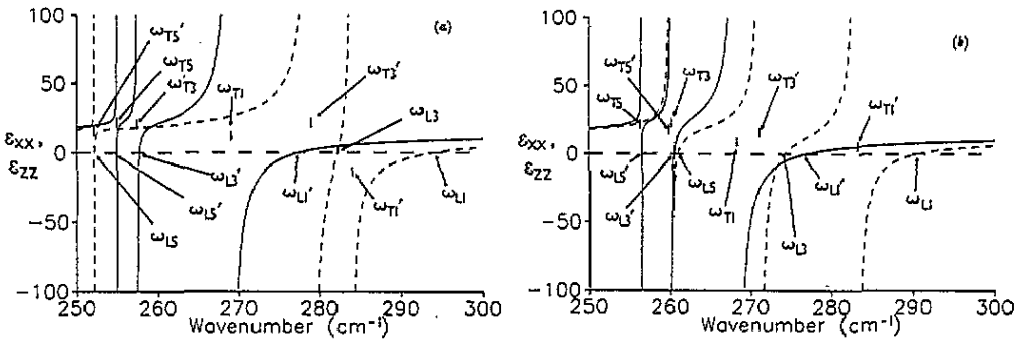

Figure 1. Principal components ϵ_{xx} (solid lines) and ϵ_{zz} (dashed lines) of the dielectric function of $(GaAs)_5/(AlAs)_5$ superlattices in the region of GaAs-like optic phonons. (*a*) Superlattice with perfect interfaces. (*b*) Superlattice having an interface roughness corresponding to W = 1.4 monolayers. All parameters are the same as those used in [16].

embellishment to the model is the incorporation, in a manner similar to that used by Chang and Mitra [19, 20] for mixed crystals, of the effects of interface roughness; since each layer may contain a mixture of atom types, an average susceptibility at each site is used. Full details are given elsewhere [16].

The principal components of the dielectric function in the GaAs region of a $(GaAs)_5/(AlAs)_5$ superlattice with perfect interfaces are shown in figure 1(*a*), calculated using the model of Samson *et al* [16] described above. In the frequency range shown, the numerical index μ on each marked mode frequency $\omega_{T\mu}$ and $\omega_{L\mu}$ is chosen to be the same as the index m which represents the number of phonon half-wavelengths within the GaAs layer. Only odd m modes contribute to the dielectric function because even m modes have no overall dipole moment. As well as the poles in ϵ_{xx} or zeroes in ϵ_{zz} which occur at the confined mode frequencies ω_{Tm} and ω_{Lm}, poles in ϵ_{zz} and zeroes in ϵ_{xx} are also marked, and labelled in the form ω'_{Tm} and ω'_{Lm} respectively. Thus above each ω_{Tm} frequency there is a corresponding ω'_{Lm} frequency at zero in ϵ_{zz} and below each ω_{Lm} frequency there is a corresponding ω'_{Tm} at a pole in ϵ_{zz}. Some useful enlightenment on the pairing of ω_{Tm} and ω'_{Lm} and of ω'_{Tm} and ω_{Lm} frequencies can be obtained by noting that (4) and (5) may be re-expressed as

$$\epsilon_{xx} = \epsilon_{yy} = \epsilon_{\infty xx} \prod_{\mu} \frac{\omega^2 - (\omega'_{L\mu})^2}{\omega^2 - \omega^2_{T\mu}} \tag{10}$$

$$\epsilon_{zz} = \epsilon_{\infty zz} \prod_{\mu} \frac{\omega^2 - \omega^2_{L\mu}}{\omega^2 - (\omega'_{T\mu})^2}. \tag{11}$$

Figure 1(*b*) shows the components for a similar superlattice with interface roughness corresponding to an error function width W of 1.4 monolayers, a value which agrees with far infrared and Raman measurements on similar samples [16]. The modes are marked in the same way as for a superlattice with perfect interfaces (the additional alloy-like modes which appear in the model [15, 16] have been ignored in this paper since they have insignificant oscillator strengths). However, the mode patterns of the atomic displacement are slightly changed from the previous case. It is evident from comparing figures 1(*a*) and 1(*b*) that the dielectric functions are noticeably influenced by interface roughness. The principal effect is

that the lower index ω_{Tm} and ω_{Lm} modes are lowered in frequency and that the higher-index modes are raised in frequency. The reason for this is discussed by, for instance, Kechrakos *et al* [21], Molinari *et al* [22], and Samson *et al* [16].

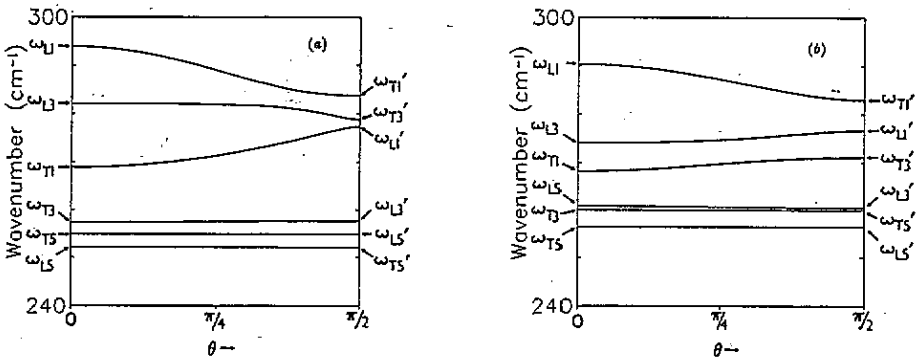

Figure 2. Angular dependence of the GaAs-like optic phonon mode frequencies of $(GaAs)_5/(AlAs)_5$ superlattices. (*a*) Superlattice with perfect interfaces. (*b*) Superlattice having an interface roughness corresponding to $W = 1.4$ monolayers.

The angular variation of the p-polarized phonon modes corresponding to (7) is plotted in figure 2. Before discussing the overall curves we consider the form of the modes present at $\theta = 0$ and $\theta = \pi/2$. At $\theta = 0$ the p-polarization modes are associated with either poles in ϵ_{xx} (the confined TO frequencies ω_{Tm}, at which $\boldsymbol{E} = 0$) or the zeroes in ϵ_{zz} (the confined LO frequencies ω_{Lm}, at which $\boldsymbol{D} = 0$). Conversely, at $\theta = \pi/2$, each mode is associated with either a zero in ϵ_{xx} (an ω'_{Lm} frequency) or a pole in ϵ_{zz} (an ω'_{Tm} frequency). These two $\theta = \pi/2$ cases can quite legitimately be described as LO and TO frequencies respectively in the same way as for $\theta = 0$. P-polarized TO modes, having $\boldsymbol{E} = 0$ and finite $\boldsymbol{D}$ transverse to the overall wavevector, propagate parallel to the interfaces (in the x direction) at poles in ϵ_{zz} (ω'_{Tm} frequencies). LO modes, having $\boldsymbol{D} = 0$ but finite $\boldsymbol{E}$ parallel to the overall wavevector, also propagate in the x direction, but at frequencies ω'_{Lm} corresponding to zeroes in ϵ_{xx}. This behaviour is obvious when one notes the similarity of (10) and (11), and it is also clear that within the macroscopic description ω_{Tm} and ω_{Lm} are no more fundamental than ω'_{Tm} and ω'_{Lm}. Although the fact that ω_{Tm} and ω_{Lm} are eigenfrequencies which directly come out of a linear chain model makes them inadvertently appear more fundamental, three-dimensional microscopic models can calculate ω'_{Tm} and ω'_{Lm} directly in a similar manner.

Since the macroscopic model described here taken no account of displacements within individual layers, some confusion may arise in the notation used to label the modes at $\theta = \pi/2$; our notation is somewhat different from that used by other authors in continuum or microscopic models. In our case the only important wavevector is a macroscopic one which applies to the whole superlattice, and at $\theta = \pi/2$ this is by definition directed along the x axis, parallel to the layers. However, within a microscopic model the confinement is implicitly associated with a local wavevector, directed perpendicular to the layers, which is considerably larger than the microscopic wavevector considered here. With respect to the microscopic wavevector, modes at ω'_{Tm} are LO-like and modes at ω'_{Lm} are TO-like, and this microscopic form of designation is usually used within other models, including continuum models. However, the x-propagating modes at ω'_{Tm} are all pure TO phonons in the macroscopic description given here, and the modes propagating at ω'_{Lm} are pure LOs.

This explains the potentially confusing phenomenon that the ω'_{Tm} frequencies tend to be higher than the ω'_{Lm} frequencies despite the fact that the former represent TO frequencies and the latter LO frequencies.

The procedure used in assigning index m to the primed frequencies ω'_{Tm} and ω'_{Lm} is inevitably somewhat arbitrary, so this index does not necessarily have any special physical significance. In particular, it should be noted that the value of m used in labelling ω'_{Tm} and ω'_{Lm} is not an indication of the number of phonon half-wavelengths confined within the GaAs layer. The x-propagating phonon at labelled frequency ω'_{T1} in the $W = 0$ case, for instance, has nearly three half-wavelengths confined within the GaAs layer. Although an effective medium model cannot directly model local displacements, this result can be anticipated from the observation that ω'_{T1} is very close to ω_{L3}. This is due to the fact that the LO_1 mode strength is considerably greater than that of LO_3 (see the effect of ω_{L3} on ω'_{T1} in the dielectric function of figure 1(a)), and is an effect which is also predicted by continuum [12] and microscopic [7, 8] models.

We now consider the frequency of the p-polarization modes in the range $0 < \theta < \pi/2$. Depending on the precise details of the forms of the dielectric functions, mode frequencies may either increase or decrease with θ. Furthermore, modes which are at ω_{Tm} frequencies at $\theta = 0$ may shift either to ω'_{Ln} or to ω'_{Tn} frequencies, where the indices m and n need not be the same, at $\theta = \pi/2$. Similarly, modes which are at ω_{Lm} frequencies at $\theta = 0$ may shift to ω'_{Tn} or ω'_{Ln} at $\theta = \pi/2$. A comparison of figures 2(a) and 2(b) shows that interface roughness can qualitatively change the behaviour of several modes in these respects. The determining factor is that ϵ_{xx} and ϵ_{zz} must be of opposite sign for the modes to exist, as is evident from (7). Since interface roughness affects the order of the various ω_{Tm}, ω_{Lm}, ω'_{Tm} and ω'_{Lm} mode frequencies, it also affects the frequency intervals within which the above condition is satisfied (see figure 1).

The macroscopic fields associated with the p-polarization modes can be determined through application of the unretarded plane wave forms of Maxwell's equations. They show that there is an $\boldsymbol{E}$ field in the wavevector direction and a $\boldsymbol{D}$ field perpendicular to it. There is no $\boldsymbol{H}$ field. These observations indicate that, within the above description, the modes are best described as phonons of mixed TO–LO character. However, other authors, using continuum models, equivalently describe such modes as hybrids of phonons with IF polaritons [12].

S-polarization modes do not vary with θ, and are TO modes occurring at ω_{Tm} frequencies, as indicated by (9). For the sake of clarity, they have not been included in figure 2.

4. Polariton modes

It is also informative to consider the general p-polarization polaritons using the full retarded form of (6). Using (6), we have determined an overall wavevector $q = (q_x^2 + q_z^2)^{1/2}$ for θ fixed at 0, $\pi/4$, and $\pi/2$. The results of these calculations for the superlattice corresponding to that represented in figure 1(b) are shown in figure 3. For $\theta = 0$, (6) reduces to $q^2 = q_z^2 = \epsilon_{xx}\omega^2/c^2$, and this is shown as figure 3(a). Note that using the above formalism only transverse modes are considered at this angle. However, dispersionless longitudinal modes exist at the ω_{Lm} frequencies and could be drawn as horizontal lines at these frequencies. A similar situation exists at $\theta = \pi/2$, as shown in figure 3(c). Here only ϵ_{zz} is used in the formalism, leading only to transverse modes as before. In a similar way to the $\theta = 0$ case, horizontal lines corresponding to longitudinal modes could be drawn at ω'_{Lm} frequencies. Figure 3(b) represents the situation when θ takes a value of $\pi/4$. All

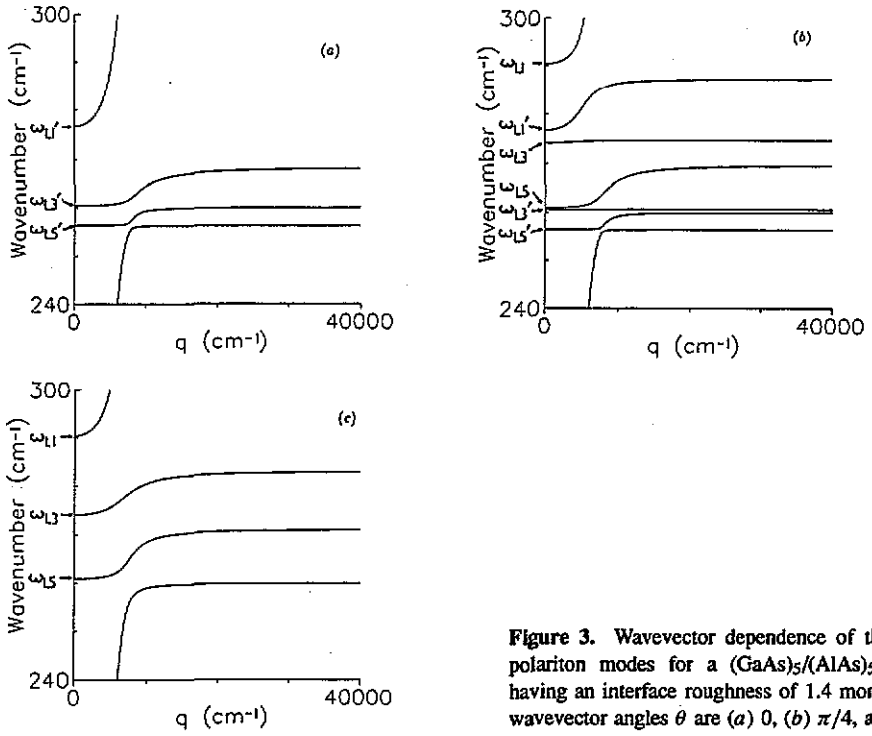

Figure 3. Wavevector dependence of the GaAs-like polariton modes for a $(GaAs)_5/(AlAs)_5$ superlattice having an interface roughness of 1.4 monolayers. The wavevector angles θ are (*a*) 0, (*b*) $\pi/4$, and (*c*) $\pi/2$.

the modes now arise directly from applying (6), and they contain both longitudinal and transverse contributions.

As $q \to 0$, equation (6) is satisfied at the ω_{Lm} and ω'_{Lm} frequencies, and as $q \to \infty$ the solutions correspond to the unretarded case already discussed and shown in figure 2(*b*). In the intermediate polariton region it is no longer a necessary condition that ϵ_{xx} and ϵ_{zz} must be of opposite sign as was the case for the phonon modes, although at least one of these components must be positive in sign [23]. The polaritons are not therefore restricted to the reststrahl (phonon) regions of the superlattice constituents. This is because (6) is essentially a description of bulk polaritons propagating through the superlattice and this description includes modes which propagate in regions where there is no optical activity, in a similar way to those which propagate in bulk isotropic media.

5. Conclusions

The above procedure can provide an accurate determination of anisotropic phonon and polariton frequencies provided a suitable method is used for modelling superlattice dielectric functions. The examples given above use dielectric function derived from a linear chain model which considers only propagation normal to superlattice layers. However, we have shown how the results of such a simple model can be extended in order to find phonon frequencies applicable to propagation in any direction.

The method is applicable in the long-wavelength limit appropriate to experimental infrared and Raman scattering conditions. In the simple form presented above the modelling is totally macroscopic in nature, so it gives no indication of local displacements or fields. However, such information is retrievable from the original microscopic model used to

derive the dielectric functions. The resulting mode patterns are similar to those published by Gerecke and Bechstedt [24], and will be presented in a separate publication.

Acknowledgment

The authors wish to thank N C Constantinou for useful discussions.

References

[1] Pokatilov E P and Beril S I 1982 *Phys. Status Solidi* b **110** K75
[2] Camley R E and Mills D L 1984 *Phys. Rev.* B **29** 1695
[3] Huber A, Egeler T, Ettmüller W, Rothfritz H, Tränkle G and Abstreiter G 1991 *Superlatt. Microstruct.* **9** 309
[4] Hessmer R, Huber A, Egeler T, Haines M, Tränkle G, Weimann G and Abstreiter G 1992 *Phys. Rev.* B **46** 4071
[5] Haines M and Scamarcio G 1993 *Proc. NATO Advanced Research Workshop on Phonons in Nanostructures 1992* at press
[6] Ren S-F, Chu H and Chang Y-C 1988 *Phys. Rev.* B **37** 8899
[7] Bechstedt F and Gerecke H 1989 *Phys. Status Solidi* b **154** 565
[8] Rücker H, Molinari E and Lugli P 1992 *Phys. Rev.* B **45** 6747
[9] Lassnig R 1984 *Phys. Rev.* B **30** 7132
[10] Babiker M 1986 *J. Phys. C: Solid State Phys.* **19** 683
[11] Zianni X, Butcher P N and Dharssi I 1992 *J. Phys.: Condens. Matter* **4** L77
[12] Constantinou N C, Al-Dossary O and Ridley B K 1993 *Solid State Commun.* **86** 191
[13] Chu H, Ren S-F and Chang Y-C 1988 *Phys. Rev.* B **37** 10746
[14] Chu H and Chang Y-C 1988 *Phys. Rev.* B **38** 12369
[15] Samson B, Smith S R P, Foxon C T, Hilton D and Moore K J 1991 *Solid State Commun.* **78** 325
[16] Samson B, Dumelow T, Hamilton A A, Parker T J, Smith S R P, Tilley D R, Foxon C T, Hilton D and Moore K J 1992 *Phys. Rev.* B **46** 2375
[17] Agranovich V M and Kravtsov V E 1985 *Solid State Commun.* **55** 85
[18] Raj N and Tilley D R 1985 *Solid State Commun.* **55** 373
[19] Chang I F and Mitra S S 1970 *Phys. Rev.* B **2** 1215
[20] Chang I F and Mitra S S 1971 *Adv. Phys.* **20** 359
[21] Kechrakos D, Briddon P R and Inkson J C 1991 *Phys. Rev.* B **44** 9114
[22] Molinari E, Baroni S, Giannozzi P and de Gironcoli S 1992 *Phys. Rev.* B **45** 4280
[23] Dumelow T and Tilley D R 1993 *J. Opt. Soc. Am.* A **10** 633
[24] Gerecke H and Bechstedt F 1991 *Phys. Rev.* B **43** 7053